INTERNATIONAL SOCIETY FOR
SOIL MECHANICS AND
GEOTECHNICAL ENGINEERING

This paper was downloaded from the Online Library of the International Society for Soil Mechanics and Geotechnical Engineering (ISSMGE). The library is available here:

https://www.issmge.org/publications/online-library

This is an open-access database that archives thousands of papers published under the Auspices of the ISSMGE.

The paper was published in the proceedings of the 11th International Conference on Physical Modelling in Geotechnics (ICPMG2026) and was edited by Ioannis Anastasopoulos. The conference was held from June 8th to June 12th 2026 in Zurich, Switzerland.

© 2026 the Authors

The movement of shallow rectangular tunnels in soft clays under earthquake loading

N.G.L.H. Lee
University of Cambridge, Schofield Centre, Cambridge, United Kingdom, nglhl2@cam.ac.uk

S.P.G. Madabhushi
University of Cambridge, Schofield Centre, Cambridge, United Kingdom, mspg1@cam.ac.uk

ABSTRACT: Earthquake-induced ground failure can cause uplift in buoyant underground structures, including shallow tunnels. While much research has looked at the seismic response of tunnels in liquefiable soils, less attention has been given to their response in soft clays. This is of interest as structural and ground failure has also been observed in fine-grained soils in the field, owing to the degradation of their strength and stiffness with cyclic loading. As such, it is important to understand the effects of this cyclic softening on a buried structure's ability to resist uplift during an earthquake. In this study, dynamic centrifuge experiments were conducted to investigate the effects of seismic loading on a shallow rectangular tunnel buried in a soft clay. With each test, the undrained shear strength of the clay was varied, yielding differing dynamic responses. Particle image velocimetry analysis showed that the seismic response of a tunnel in soft clay is distinct from its well-investigated counterpart in sandy soils, even when tunnel uplift does occur. While similar displacement mechanisms occurred, as the clay retains some stiffness, clay above the tunnel heaved together with the tunnel, resulting in similar vertical displacements between the surface and the tunnel. Lateral movements were also significant due to the high compressibility of clay, even when uplift was minimal. These findings highlight the value in studying the seismic response of tunnels in clay, even if less critical than liquefaction in terms of uplift.

1 INTRODUCTION

With ever-growing demands for infrastructure in densely populated areas, underground space is continually being utilised for transport and utility systems. Examples include the construction of shallow tunnels for underground railway lines. In all buoyant underground structures, seismic failure can occur in the form of uplift due to earthquake-induced ground failure. Following the vertical slip model by Trautmann et al. (1985), their susceptibility to uplift can be determined by considering the vertical forces acting on it, as shown in Figure 1.

In static conditions, the buoyant force acting on a tunnel F_b is resisted by the weight of the tunnel F_t and the overlying soil F_s, resulting in a ground bearing pressure beneath the tunnel invert F_{gbp}. The factor of safety FoS of a tunnel against uplift can be expressed by the following equation:

$$FoS = \frac{F_t + F_s}{F_b} \quad (1)$$

Under dynamic conditions, excess pore pressure F_{epp} may be generated, and the net upward force will be resisted by the shear resistance along the tunnel side walls F_{sw} and the soil along a slip plane F_{sp}.

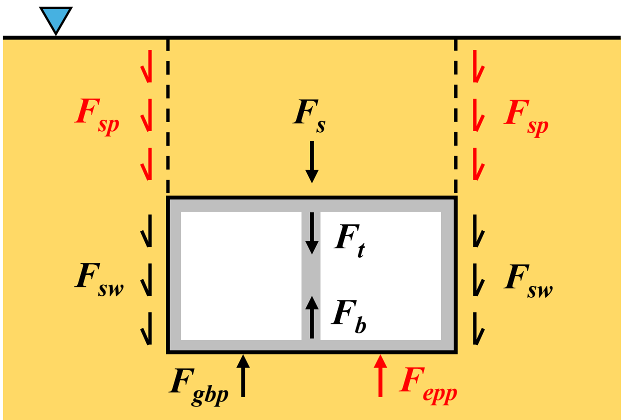

Figure 1. Vertical forces on a tunnel buried in saturated soil.

The most critical case involves the liquefaction of loose, saturated, sandy soils, where rapid cyclic loading results in a significant loss in strength and stiffness. In seismically active cities founded on liquefiable soil, several cases of liquefaction-induced uplift has been observed in shallow tunnels and other light underground structures (Tokimatsu et al., 2013;

Franco et al., 2018). This has led to considerable research on the effects of earthquake-induced liquefaction on buried structures (Tsinidis, 2020). In the centrifuge, research has been carried out considering tunnel floatation in a single soil stratum (Chian et al., 2014; He et al., 2025), as well as in more complex profiles based on field conditions (Yang et al., 2004; Chou et al., 2011). These studies mostly focused on saturated sand strata, where the loss of soil stiffness was driven by the buildup of excess pore pressures F_{epp} and consequent liquefaction.

In clays, strength and stiffness degradation under cyclic loading is also possible, although generally to a lesser degree. This process is known as cyclic softening (Idriss et al., 1978) and has also played a significant role in structural and ground failure, e.g., during the 1999 Chi-Chi Earthquake (Tsai et al., 2014) and the 1999 Kocaeli Earthquake (Okur et al., 2008). With respect to Figure 1, this would affect the shear resistance of the clay F_{sp}. However, the high strain rate associated with seismic loading has also been shown to increase undrained shear strength, possibly compensating for the degradation associated with cycling (Ishihara et al., 1983; Lefebvre & LeBouef, 1987). There is a need for further experimental studies that explore the displacement response of a buried structure due to cyclic clay strength degradation, particularly under the rapid dynamic conditions expected during an earthquake. The type of cyclic loading (earthquake, wind, wave) and laboratory testing method (triaxial vs direct simple shear) has been shown to affect cyclic shear strength (Andersen, 2009).

This presented an opportunity to study the seismic behaviour of a soft clay in the centrifuge, and its impact on the resistance of a buried tunnel against vertical and lateral movement. The highly nonlinear stress-strain behaviour of soil can be captured without making prior assumptions about failure mechanisms (Schofield, 1980; Madabhushi, 2014). This study aimed to investigate the following: how would a shallow tunnel behave in a clay that has the potential for cyclic softening during shaking? Given the differences in flow characteristics of a softened clay compared to liquefied sand, would its movement patterns differ during uplift? Could its high compressibility result in notable lateral movements, even if resistance to uplift is maintained?

2 METHODOLOGY

Two dynamic centrifuge tests were conducted using the Schofield Centre Turner beam centrifuge at the University of Cambridge. This experimental method has been used extensively in geotechnical investigations: when subject to an acceleration of *N* g, a reduced 1:*N* scale physical model experiences the stresses and strains expected from a full-scale prototype (Schofield, 1980; Madabhushi, 2014).

To observe movements in the tunnel and surrounding clay in plane strain conditions, a rigid window container was used with dimensions 500 x 360 x 250 mm. With consideration of boundary effects, an acceleration of 80 g was decided to produce a prototype of a 4 x 8 m rigid double box concrete tunnel, representing a metro tunnel with two railway lines, buried in a 20 m thick clay stratum.

2.1 Model design

The objective of the tests was to induce sufficient strength and stiffness degradation in a volume of clay under cyclic earthquake loading for a shallow buried tunnel to undergo dynamic movements. In consideration of the critical uplift failure mechanism, the main design parameters of these tests were as follows:

- the cover depth of the tunnel
- the undrained shear strength of the overlying clay

As a first step to provide a baseline for structural failure under the "worst" conditions possible, the tunnels were wished-in-place in a single clay stratum, without the remediation measures expected in the field (e.g., overlying the tunnel with a denser backfill). Table 1 presents these key properties for the two centrifuge models, and their resulting static *FoS* against uplift. The tunnel cover depth was maintained across the models, while the undrained shear strength of the clay was varied. These two models are hereby referred to as "soft clay" and "very soft clay". Although the cover depth was consistent between the two models, the different unit weights of the soft and very soft clay result in varying static *FoS* values.

Table 1. Model design parameters.

Model ID	**Tunnel cover depth (*m*)**	**Overlying clay s_u (*kPa*)**	**Static *FoS***
Soft clay	3.2	11.0	1.18
Very soft clay	3.2	3.4	1.13

2.2 Model preparation

As it is difficult to scale reinforced concrete (Madabhushi, 2014), the concrete prototype tunnel was modelled using equivalent aluminium sections, such that its bending stiffness per unit length EI was

N^3 times smaller than the concrete prototype. Scaling was based on the weak axis EI_{xx} in consideration of vertical uplift. Table 2 summarises the properties of the concrete tunnel prototype and the aluminium model. A flexibility ratio F of 0.1 to 0.3 was determined for the soft and very soft clays used in this study (Wang, 1993), indicating that the tunnel is rigid relative to its surrounding soil (F<1). This was confirmed by the PIV analysis.

Table 2. Prototype and equivalent model tunnel properties.

Tunnel parameter	Prototype	Model at 80 g
Height (**m**)	4.064	
Width (**m**)	8.128	
Wall thickness (**m**)	0.460	0.128
Young's Modulus E (**MPa**)	25	70
Flexural stiffness EI_{xx} (**MNm²/m**)	0.729×10^6	
Axial stiffness EA (**MN/m**)	3.314×10^5	2.821×10^5

The double box tunnel model was made by bolting two hollow 6082 T6 aluminium alloy sections, with all joints sealed with silicon for waterproofing. Polytetrafluoroethylene (PTFE) sections were added at each end to reduce friction between the tunnel and container, with movement markers applied on its front face as shown in Figure 2. MEMS accelerometers were also superglued onto the tunnel to measure horizontal and vertical accelerations.

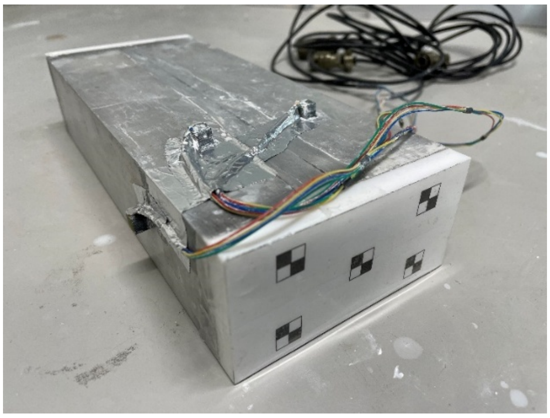

Figure 2. Aluminium model tunnel.

Laboratory-grade speswhite kaolin clay was used in this study, as commonly adopted in centrifuge experiments due to its relative permeability minimising the consolidation time required in flight. Table 3 presents their relevant index properties recently determined at Schofield Centre (Chan, 2020).

For each model, the clay layer was prepared using both incremental mechanical loading and suction-induced seepage consolidation outside the centrifuge (Robinson et al., 2003), from an initial slurry state at approximately twice the liquid limit. This helped achieve an increasing strength profile expected in the field. Pre-consolidation was done directly in the window container with its front face replaced by a rigid aluminium plate, and the final top load applied to the soft and very soft clay models were 80 kPa and 40 kPa, respectively. In both models, a target suction pressure of -70 kPa was applied at the base of the container. Prior to consolidation, water pump grease was applied to the back and side walls of the container, with clear silicon grease on the front. This minimised the effects of friction during both consolidation and shaking.

After consolidation, the clay layer was trimmed at the surface to its designed height, and the tunnel was installed through the front face by removing clay along the depth of its cross section. Piezo-electric accelerometers and pore pressure transducers were installed at the free-field and below the tunnel, as shown in Figure 3. Finally, dyed black Hostun HN31 sand was applied on the front face as seeding for PIV analysis on the clay body (White et al., 2003).

Table 3. Index properties of speswhite kaolin clay.

Parameter	Value
Liquid limit LL (%)	75.0
Plasticity index PI (%)	41.8
Specific gravity G_s	2.61
Compression index λ	0.19
Swelling index κ	0.07

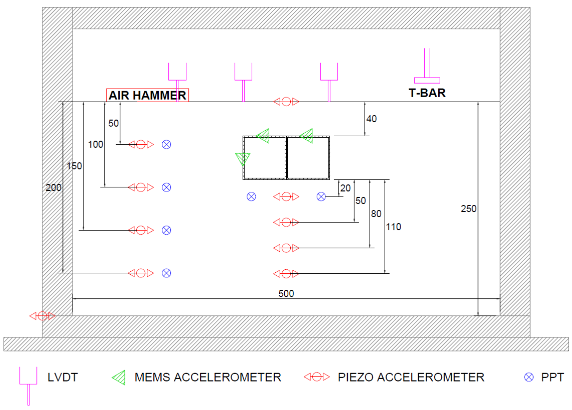

Figure 3. Model schematic.

2.3 In-flight characterisation and test sequence

Once accelerated to 80 g, the models were given 60 minutes to consolidate, after which the undrained shear strength s_u and small-strain stiffness G_0 of the clay was determined using the T-bar (Stewart and Randolph, 1991) and air hammer test (Ghosh and Madabhushi, 2002), respectively. Pore pressure measurements were used to estimate the effective stress of the clay with depth, enabling predictions of these strength and stiffness parameters as shown in Figure 4.

The s_u profiles obtained from the T-bar compared reasonably well with estimations based on effective stress, plasticity and OCR (Wroth, 1984). This was determined by applying the standard T-bar bearing factor of 10.5, recommended for general use in deep penetration conditions (Randolph, 2004), to the measured pressure on the penetrometer. Shear wave velocity V_s values obtained from the air hammer test also yielded G_0 ranges around those by Hardin and Drnevich (1972) as well as Viggiani and Atkinson (1995). Overall, these results validated the effectiveness of the 1 *g* consolidation methods to achieve the increasing profiles with depth, as well as the low strength ranges desired in the surrounding clay.

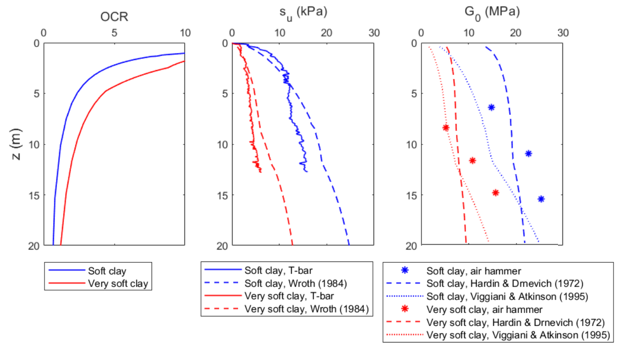

Figure 4. OCR, undrained shear strength and small-strain stiffness profiles.

The models were then subjected to earthquake motions of increasing intensity using the servo-hydraulic shaker designed by Madabhushi et al. (2012). Table 4 summarises the peak ground accelerations recorded in each model. Apart from EQ1 where slightly different sine sweep motions were applied, very consistent shaking amplitudes were measured in both models.

Table 4. Earthquake sequence.

ID	Type	Frequency (*Hz*)	PGA (*g*) Soft clay	PGA (*g*) Very soft clay
EQ1	Sine sweep	100 - 0	0.06	0.04
EQ2	Kobe	-	0.17	0.17
EQ3	Sine (15 cycles)	1	0.11	0.11
EQ4			0.18	0.18
EQ5			0.24	0.24

"Simple" sinusoidal base motions have been criticised for overly emphasising certain aspects of the soil's response (Kutter, 1995). However, they are not unrealistic either, as shown from the 1985 Mexico City and 1989 Loma Prieta earthquake (Schofield & Steedman, 1992). In this study, the sinewave motions (EQ3 to EQ5) with a maintained frequency allowed for clear trends in soil and tunnel behaviour to be observed with respect to shaking amplitude.

3 RESULTS AND DISCUSSION

In both models, the effects of cyclic softening were observed during the 0.1 g < PGA < 0.25 g series of 15-cycle sinewave motions fired at 1 *Hz* (EQ3 to EQ5). While significant tunnel uplift was only observed in the very soft clay model, lateral movements were considerable in both models. The following sections detail the deformations observed in both the tunnel and the surrounding clay, as well as the changes in acceleration and pore pressure associated with cyclic softening and tunnel uplift.

3.1 Dynamic soil response

3.1.1 Acceleration

The effects of cyclic softening are observed as a gradual attenuation of horizontal accelerations over shaking cycles. An example of this acceleration time history is shown in Figure 5. This is also presented along the depth of the clay layer in terms of amplification ratio in Figure 6, which includes the response at the free-field as well as the tunnel axis. The amplification profile along the tunnel axis also includes the horizontal acceleration measured directly on the tunnel crown.

Before any degradation occurs, there is an initial continuous amplification of accelerations upward along the clay layer. However, during a sufficiently strong earthquake, the shear strength of the clay is exceeded by the mobilised shear stresses, and the clay yields. These shear stresses generated can be estimated from acceleration measurements according to Garala & Madabhushi (2018). Depending on the strength of the overlying clay, these limited accelerations can then either amplify or attenuate upward.

In the soft clay, cyclic softening was observed at the shallowest accelerometer in the free field at z/H = 0.14, and below the tunnel at z/H = 0.43. However, at this tunnel axis, amplification persisted upwards, with an increased acceleration initially measured on the tunnel crown, before the reduction observed over time. This indicated that cyclic softening occurred at the tunnel level as well.

In the very soft clay, cyclic softening was more pronounced. At the free field, significant attenuations were observed over cycles at $z/H = 0.2$ during EQ3, as well as at $z/H = 0.4$ from EQ4 onwards. Similar observations were made at the tunnel axis, and the significant reduction in horizontal acceleration at the tunnel crown corresponded with large uplift (shown in subsequent sections). Measurements on the clay surface above the tunnel showed that they largely followed the acceleration response of the tunnel as they heave together. This will be shown in Section 3.2.

The amplification profile shows a progressive degradation trend in clay accelerations from the initial point of yielding. With increasing shaking amplitude, there is an increase in both the degree of attenuation at a given depth over cycles, as well as in the size of the attenuation zone with depth. The tendency of the clay to either amplify or attenuate accelerations with depth and time has considerable influence on the accelerations experienced by the tunnel. In fact, the initial amplification ratio at the tunnel crown significantly varies between the soft (1.3 to 1.5) and very soft clay (0.2 to 0.8) from EQ3 to EQ5.

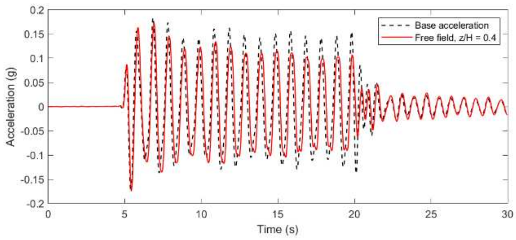

Figure 5. Attenuation of accelerations in very soft clay during EQ4.

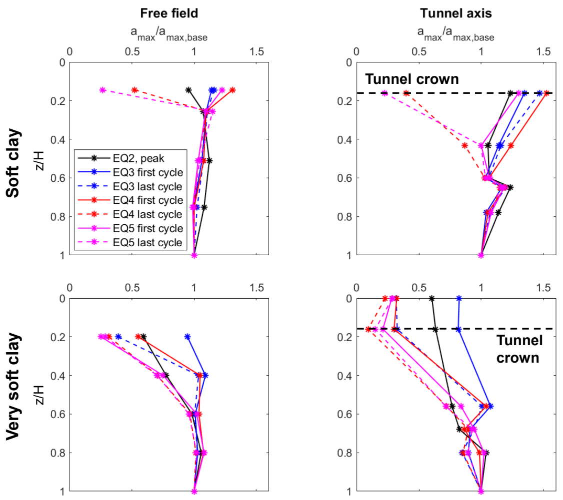

Figure 6. Amplification ratio at free field and tunnel axis.

3.1.2 Pore pressure

The cyclic degradation of soft clays is also associated with excess pore pressure developments (Andersen et al., 1988). Figure 7 presents the pore pressure readings measured below the tunnel in the soft and very soft clay, along with the vertical displacements of the tunnel measured from EQ3 to EQ5.

In the soft clay, the gradual accumulation of pore pressure increases with shaking intensity. This is combined with the fatigue loading that results in the gradual destructuration and weakening of the clay (LeBoeuf et al., 2016), as observed in the acceleration response. In the very soft clay, dynamic pore pressure initially follows the trend observed in the soft clay. However, suction is induced as the tunnel ratchets upward above the clay, offsetting this buildup in excess pore pressure. This results in an eventual downward trend in excess pore pressure corresponding with the onset of tunnel uplift.

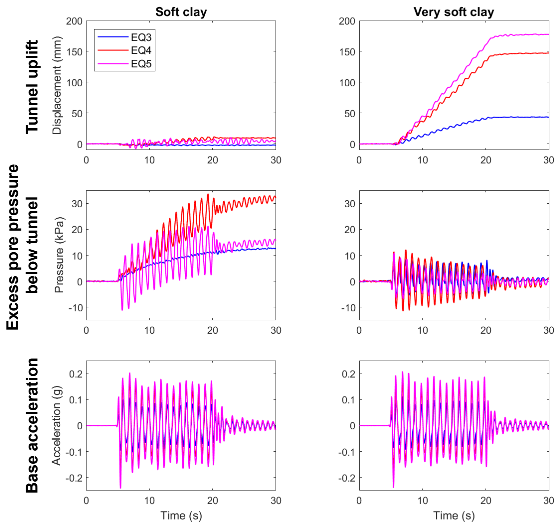

Figure 7. Pore pressures recorded under the tunnel corresponding to variable uplift.

The dynamic excess pore pressures captured from EQ3 to EQ5 range from 10-30 kPa in the soft clay. At this depth, the effective stress estimated in the clay prior to shaking was around 66 kPa. This would suggest a maximum excess pore pressure ratio of around 0.45, which appears similar to values obtained from cyclic triaxial tests on soft clays (Matasovic & Vucetic, 1992). However, there is some level of uncertainty in these recorded pore pressures. In dynamic tests, vibrations of the transducer itself relative to the soil body can also be registered as dynamic pressure. These cyclic pressures were not recorded for the smallest earthquake (EQ3) in the soft clay, which could suggest a decoupling (or detachment) between the transducer and the soil during subsequent earthquakes, although an overall increase in pore pressure over time was still observed. Further investigation is required to ascertain the true nature of these dynamic excess pore pressures; however, long-term dissipation after shaking suggests that the overall excess pore pressure buildup was truly recorded.

3.2 Dynamic tunnel response

The soil's dynamic response showed that cyclic softening occurred in the surrounding clay. With respect to the vertical forces shown in Figure 1, these implied a reduction in F_{sp} and a buildup of F_{epp}, respectively, giving cause for tunnel uplift. This section details the dynamic movements of the tunnel and surrounding clay determined from GeoPIV-RG analysis (Stanier et al., 2016), focusing on EQ4, where significant uplift was first observed in the very soft clay model (see Figure 7).

3.2.1 Tunnel displacements

In all cases, significant tunnel movement was observed with the onset of shear failure in the surrounding clay. Figure 8 presents the vertical and horizontal movements of the tunnel during EQ4. The vertical and horizontal displacements are also compared against those of the overlying clay surface and the adjacent soil, respectively.

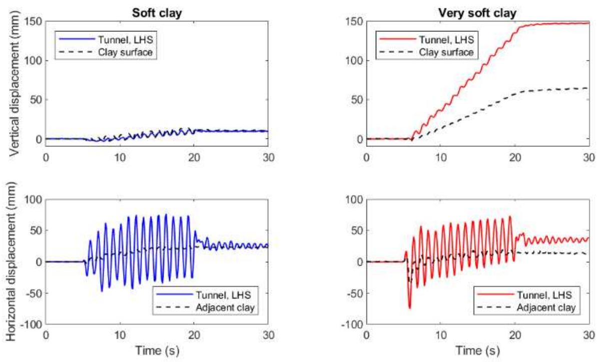

Figure 8. Tunnel vertical and horizontal displacements during EQ4.

In the soft clay, the tunnel underwent minimal uplift, although some cyclic vertical displacements were captured both at the tunnel and the clay surface. However, significant uplift was observed in the very soft clay, following the ratcheting response seen in previous studies on the dynamic behaviour of shallow rectangular tunnels. The rate of uplift was quite uniform with shaking cycles, and resulted in a total uplift of approximately 150 mm (4.7% of the tunnel's cover depth) that was maintained after shaking concluded. This was also followed by uplift at the overlying clay surface, although to a lesser extent.

Regardless of uplift magnitude, significant lateral displacements were seen in the tunnel. The magnitudes of these displacements were very large (± 50 mm) and were significantly higher than that of the adjacent clay. This could be due to the high compressibility of the clay that results in the tunnel being able to push considerably into the adjacent clay. This is quite concerning, even when compared to similar configurations in liquefiable sand; for a similar range in static *FoS* against uplift, these lateral movements measured in soft clays are approximately twice of those in loose saturated sand, even when liquefaction caused much larger tunnel uplift (He et al., 2025).

3.2.2 Associated clay displacement

While not associated with tunnel uplift, flow-type failure induced by cyclic softening has been observed in saturated clayey soils during earthquake loading in the field (Tsai et al., 2022; Cetin et al., 2024). With respect to tunnel uplift, this is typically observed in liquefied sands through circular displacement "loops" on both sides of the tunnel. This was investigated in the soft and very soft clay as shown in the vector plots in Figure 9.

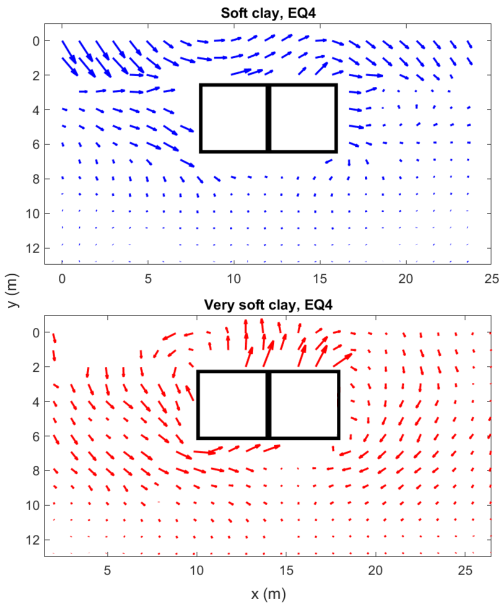

Figure 9. Soil vector plots for EQ4.

In the soft clay, considerable displacements were observed within a wide inclined zone spreading out from the base of the tunnel to the clay surface. This could suggest a longer shear plane than the vertical ones assumed in Figure 1, and could be why the tunnel resists uplift in spite of cyclic softening. This would be similar to the mechanism considered by Chou et al. (2011) concerning the shear failure of soft clay beneath the BART tunnel. In this configuration, the clay surface largely follows the tunnel's limited uplift, while settlement occurs at either side of the tunnel up to the depth of the tunnel crown.

In the very soft clay, the tunnel undergoes significant uplift relative to the surrounding clay. However, unlike the typical displacement loops observed in sand, the overlying clay is not pushed aside. Instead, the block of clay directly above heaves together with the tunnel, resulting in considerable vertical displacements at the surface as well. While the circular loops are present, they are much smaller than the circular flow mechanism observed in liquefied soil as the clay does not lose all stiffness. This could suggest a greater risk of surface heave for a buried structure uplifting in clay. Furthermore, as the tunnel uplifts, the clay is unable to fill the resulting cavity underneath, leaving a uniform gap between the base of the tunnel and the clay as shown in Figure 10. In liquefied soil, the infill of this void has been seen to drive additional upward displacement (Yang et al., 2004; Chian et al., 2014) as soil wedges under the lower corners of the shaking tunnel.

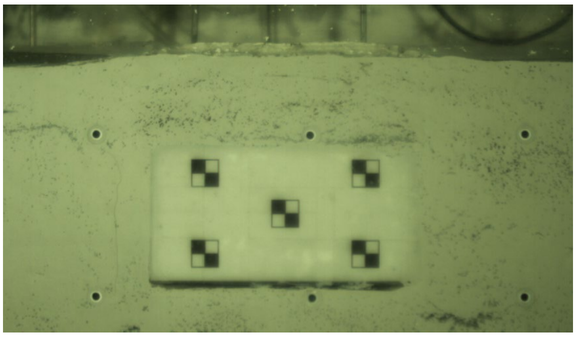

Figure 10. Surface heave and gap below tunnel in very soft clay from EQ4.

4 CONCLUSIONS

This study investigated the vertical and lateral movements of a rectangular tunnel in soft clay under earthquake loading, and the associated displacements of the surrounding clay. Two dynamic centrifuge tests were conducted on tunnels buried a shallow depth in speswhite kaolin clay models with varying low undrained shear strength profiles.

Although the initial design approach considered uplift due to cyclic softening, significant lateral movements were consistently observed as well. These persisted across two modes of failure observed with varying degrees of vertical tunnel movement. In contrast to liquefied sand, where tunnel uplift is of primary concern, there is a greater tendency for lateral movement in soft clays. For tunnels passing through multiple soil strata, this could cause significant damage to circumferential joints as individual segments undergo varying ratcheting responses, both vertically and horizontally.

These findings show that while less severe than its sister response in liquefiable sandy soils in terms of uplift, the seismic response of a soft clay-tunnel system is unique, even as no uplift occurs. It is worth investigating this further, as well as the seismic response of mitigation measures that are largely designed to resist the upward movement of a buoyant tunnel.

ACKNOWLEDGEMENTS

The authors are grateful for the support of the technicians at Schofield Centre in the preparation and execution of this work.

REFERENCES

Andersen, K. H. (2009). Bearing capacity under cyclic loading – offshore, along the coast, and on land. *Canadian Geotechnical Journal*, 46(5), 513-535.

Andersen, K. H., Kleven, A., & Heien, D. (1988). Cyclic soil data for design of gravity structures. *Journal of Geotechnical engineering*, *114*(5), 517-539.

Cetin, K. O., Soylemez, B., Guzel, H., and Cakir, E., (2024). Soil liquefaction sites following the February 6, 2023, Kahramanmaraş-Türkiye earthquake sequence. *Bulletin of Earthquake Engineering*, https://doi.org/10.1007/s10518-024-01875-3

Chan, D. (2020). *Long-term basement heave in over-consolidated clay* [Doctoral dissertation, University of Cambridge].

Chian, S. C., Tokimatsu, K., and Madabhushi, S.P.G. (2014). Soil liquefaction–induced uplift of underground structures: physical and numerical modelling. *Journal of Geotechnical and Geoenvironmental Engineering*, 140(10), 1–18. https://doi.org/10.1061/(ASCE)GT.1943-5606.0001159

Chou, J.C., Kutter, B.L., Travasarou, T., & Chacko, J.M. (2011). Centrifuge modeling of seismically induced uplift for the BART transbay tube. *Journal of Geotechnical and Geoenvironmental Engineering*, 137, 754-765. https://doi.org/10.1061/(ASCE)GT.1943-5606.0000489

Franco, G., Stone, H., Ahmed, B., Chian, S.C., Hughes, F., Jirouskova, N., Kaminski, S., Lopez, J., van Drunen, N., Hutt, C. M., and Querembas, M. (2018). The *M_w7.8 Muisne Ecuador earthquake of 16 April 2016 : a field report by EEFIT*. EEFIT, The Institution of Structural Engineers. https://www.istructe.org/resources/report/eefit-mission-muisne-ecuador-earthquake/

Garala, T. K., & Madabhushi, G. S. (2019). Seismic behaviour of soft clay and its influence on the response of friction pile foundations. *Bulletin of Earthquake Engineering*, *17*(4), 1919-1939.

Ghosh, B. and Madabhushi, S. P. G. (2002). An efficient tool for measuring shear wave velocity in the centrifuge. In *Proceedings of the International Conference on Physical Modelling in Geotechnics,*119–124, Balkema, Rotterdam.

Hardin, B. O. and Drnevich, V. P. (1972). Shear modulus and damping in soils: design equation and curves. *Journal of the Soil Mechanics and Foundations Division*, 98(7), 667-692.

He, Z., Lee, N. G. L. H., and Madabhushi, S. P. G. (2025). Seismic behaviour of shallow cut-and-cover tunnels. *Soils and Foundations,* 65(3), 101612. https://doi.org/10.1016/j.sandf.2025.101612

Idriss, I. M., Dobry, R., and Singh, R. D. (1978). Nonlinear behavior of soft clays during cyclic loading. *Soils and Foundations*, 33(1), 182-191.

Ishihara, K., Akira, N., and Mano, R. (1983). Residual strain and strength of clay under seismic loading. *Proceedings of the 4th Canadian Conference on Earthquake Engineering*, 602-613.

Kutter, B. L. (1995). Recent advances in centrifuge modeling of seismic shaking. *Proceedings of the Third International Conference on Recent Advances in Geotechnical Earthquake Engineering and Soil Dynamics*, St. Louis, Missouri.

LeBoeuf, D., Duguay-Blanchette, J., Lemelin, J. C., Péloquin, E., and Burckhardt, G. (2016). Cyclic softening and failure in sensitive clays and silts. *Proceedings of the 1st International Conference on Natural Hazards and Infrastructure, Chania, Greece*.

Lefebvre, G. and LeBoeuf, D. (1987). Rate effects and cyclic loading of sensitive clays. *Journal of Geotechnical Engineering*, ASCE, 113(5), 476-489.

Madabhushi, S.P.G. (2014). *Centrifuge modelling for civil engineers*. CRC Press.

Madabhushi, G. S., Haigh, S. K., Houghton, N. E., and Gould, E. (2012). Development of a servo-hydraulic earthquake actuator for the Cambridge Turner beam centrifuge. *International Journal of Physical Modelling in Geotechnics*, 12(2), 77-88.

Matasovic, N. and Vucetic, M. (1992). A pore pressure model for cyclic straining of clay. *Soils and Foundations*, *32*(3), 156-173.

Okur, V., Altun, S., and Ansal, A. (2008). Cyclic failure of fine-grained soils during the 1999 Kocaeli earthquake. *Geotechnical Earthquake and Engineering and Soil Dynamics IV Congress 2008*, Sacramento, California. https://doi.org/10.1061/40975(318)87

Randolph, M. F. (2004). Characterization of soft sediments for offshore applications. In *Proceedings of the 2nd International Conference on Site Characterization*, Millpress, Rotterdam, 209-232.

Robinson, R. G., Tan, T. S., and Lee, F. H. (2003). A comparative study of suction-induced seepage consolidation versus centrifuge consolidation. *Journal of Geotechnical Testing*, 26(1), 1-10. https://doi.org/10.1520/GTJ11109J

Schofield, A. N. (1980). Cambridge geotechnical centrifuge operations. *Geotechnique,* 30(3), 227-268.

Schofield, A. M. and Steedman, R. S. (1992). *Development of a WES Centrifuge* (No. 2602R004).

Stanier, S. A., Blaber, J., Take, W. A., & White, D. J. (2016). Improved image-based deformation measurement for geotechnical applications. *Canadian Geotechnical Journal,* 53(5), 727-739.

Stewart, D.P. and Randolph, M.F. (1991). A new site investigation tool for the centrifuge. In *Proceedings of the International Conference on Centrifuge Modelling, Centrifuge '91*, Boulder, Colorado, 13–14 June 1991. 531–538, Balkema, Rotterdam.

Tokimatsu, K., Suzuki, H., Katsumata, K., and Tamura, S. (2013). Geotechnical problems in the 2011 Tohoku Pacific earthquakes*. International Conference on Case Histories in Geotechnical Engineering*, 2.

Trautmann, C. H., O'Rourke, T. D., and Kulhawy, F. H. (1985). Uplift force-displacement response of buried pipe. *Journal of Geotechnical Engineering*, 111(9), 1061-1076.

Tsai, C. C., Mejia, L. H., and Meymand, P. (2014). A strain-based procedure to estimate strength softening in saturated clays during earthquakes. *Soil Dynamics and Earthquake Engineering*, 66, 191-198.

Tsai, C. C., Yang, Z. X., Chung, M. H., and Hsu, S. Y., (2022). Case study of large-scale levee failures induced by cyclic softening of clay during the 2016 Meinong earthquake. *Engineering Geology,* 297, https://doi.org/10.1016/j.enggeo.2022.106518

Tsinidis, G., de Silva, F., Anastasopoulos, I., Bilotta, E., Bobet, A., Hashash, Y. M. A., He, C., Kampas, G., Knappett, J., Madabhushi, S. P. G., Nikitas, N., Pitilakis, K., Silvestri, F., Viggiani, G. M. B., & Fuentes, R. (2020). Seismic behaviour of tunnels: from experiments to analysis. *Tunnelling and Underground Space Technology*, 99, 103334. https://doi.org/10.1016/j.tust.2020.103334

Viggiani, G. M. B. and Atkinson, J.H. (1995). Stiffness of fine-grained soil at very small strains. *Géotechnique*, 45(2), 249-265. https://doi.org/10.1680/geot.1995.45.2.249

Wang, J. N. (1993). *Seismic design of tunnels: a simple state-of-the-art design approach*. Parsons Brinckerhoff.

White, D. J., Take, W. A., and Bolton, M. D. (2003). Soil deformation measurement using particle image velocimetry (PIV) and photogrammetry. *Geotechnique*, 53(7), 619-631.

Wroth, C.P. (1984). The interpretation of in situ soil tests. *Géotechnique*, 34(4), 449-489. https://doi.org/10.1680/geot.1984.34.4.449

Yang, D., Naesgaard, E., Byrne, P. M., Adalier, K., and Abdoun, T. (2004). Numerical model verification and calibration of George Massey Tunnel using centrifuge models. *Canadian Geotechnical Journal*, 41(5), 921–942. https://doi.org/10.1139/t04-039